ELSEVIER

Analysis on biological importance of antiseptic drug, O-Benzyl hydroxylamine, by the application of spectroscopic and theoretical tools

Check for updates

A. Abbas Manthiri [a,b], Gene George [a], S. Ramalingam [c,*], R. Aarthi [d]

[a] Department of Physics, T.B.M.L. College, Porayar, Tamilnadu, India
[b] Department of Physics, Jamal Mohamed College, Tiruchirappalli, Tamilnadu, India
[c] Department of Physics, A.V.C. College, Mayiladuthurai, Tamilnadu, India
[d] Department of Physics, ST. Theresa's Arts and Science College, Tharangambadi, Tamilnadu, India

ABSTRACT

Biological importance of antiseptic drug; O-Benzyl hydroxylamine was explored using QSAR studies for ultimate usage for treating fungal infections. In this research work, the molecular spectroscopic tool and theoretical calculation method of analysis. The data acquired from both tools were evaluated and compared to validate structural and vibrational characteristics. Mulliken charge displacement around molecular site in order for exploring electronic properties to find out the cause of inducement of drug potential. The Lipinski rule of five was evaluated for the measurement of biological importance of the drug compound. The lipophilicity and topological surface area of the drug was monitored for determining biological process activity. The partial involvement of compositional bonds of the molecule was appraised for influential vibrational characteristics. The chemical environment for making chemical property was monitored from the uniform and asymmetrical chemical shift of core and allied carbons. The resultant oscillating potential orientation in the molecular site was identified and the residing zones were recognized to find out the origin of drug potential. The occurrence of CT complex process was studied and the CTC was found to be CC and C–N for generating drug activeness. The enhancement of hyper active polarization was measured in first and second order from which the charge level pulling on different entities were observed for ensuring the biological affinity of the compound. The enantiomer characteristics were thoroughly studied to measure the level of toxicity.

1. Introduction

The phenol is basically drug compound and particularly it is widely used as an antiseptic. Normally, the Phenol is medically used as a preservative in special type of vaccines [1]. Here, the phenol is converted in to hydroxyl methyl benzene and it is directly substituted with amine group and formed the O-Benzyl hydroxylamine. Usually, when N–O bonded compound has peculiar structure which is significant type of chemical species due to their special biological activity [2]. In this case, hydroxyl methyl group is protected by amine group which enhances the medical activity and thereby the species has multidimensional pharmaceutical activity [3]. The present compound has attracted many organic scientists for the preparation of pharmaceutical products due to the biological activeness.

Recent days, the hydroxylamine derivatives intermediate are having much attention due to usage of the preparation of Aziridines [4],

b-Amino acids and Isoxazolidinones [5]. Since, the present chemical species is powerful inhibitors and have pharmacological and therapeutic effects; it is chemically used for the preparation of antibiotic, antiseptic and anti fungal compounds which provides better results when compared with other similar compounds [6, 7].

By screening the literatures as well as available pharmaceutical resources, it was clear that, the present drug; O-Benzyl hydroxylamine is fundamentally having drug potential and the medical data explained that, the part of the pharmaceutical applications of the compound was only briefed. It is necessary to explore the entire drug potential of the present compound in order to use this chemical species for fabricating new novel multifunctional drug. It is well known that, by examining the drug properties of the chemical species, the application of the drug compound can be determined. In order to expose biological property of the compound, biological as well as structural activity properties are to be studied. In this way, it is an attempt to study the entire physic-

chemical properties making use of molecular spectroscopic and computational tools. Here, the molecular spectroscopic tools have been used in non conventional way to analyze the present compound.

2. Experimental

The present drug compound; O-Benzyl hydroxylamine is obtained from Chemical industry, USA, it is well known that, the compound is under good spectroscopic grade and it can be used for recording the spectra.

- The FT-IR spectral pattern of the compound was recorded using a Bruker IFS 66V with high resolution vib-rot spectrometer with different scanning speed [7].
- The FT-Raman spectral sequence of present compound was recorded using Bruker spectrometer adopted with FTR instrument with Raman module equipped with a Nd:YAG laser source being opterated at 1.068 μm line width with 500 mW power.
- The high resolution ^{1}HNMR and ^{13}CNMR spectra were recorded using 300 MHz and 75 MHz NMR spectrometer with high magnetic gradient.
- The UV-Vis spectra were recorded in solid phase in the region of 200 nm–800 nm, with the scanning interval of 0.22 nm, using the UV-1800 series instrument.

2.1. Biological parameter observation

The biological parameters and QSAR values have been experiential from Molinspiration apparatus and it is broad series of cheminformatics tool that can be used for molecule manipulation and dispensation, as well as SMILES and SD file translation, normalization of molecules, generation of tautomers, molecule fragmentation, calculation of various molecular properties required in QSAR, molecular modeling and drug design, high quality molecule depiction calculation and bioactivity prediction.

HyperChem is a compact molecular modeling programmable tool and it has modules based on Molecular Mechanics (MM) methods with several force fields and also modules for electronic structure calculations at semiempirical and ab-initio levels. The chemical tool is also used for Computing the structure and stability of molecules using MMX method.

3. Calculation

In computational part, all the parameters have been calculated by performing quantum chemical computations on Gaussian 16 D. 01 version software program in IMAC computer [8]. The spectral pattern and optimized geometrical parameters were computed at the true geometry which was found after performing structure stability scan. The associated properties related with electronic spectra; NBMO and frontier orbital sequence were calculated by adopting time-dependent SCF method with best fit basis set. The ^{1}H and ^{13}C Nuclear Magnetic Resonance isotropic chemical shifts were calculated by Gauge Independent Atomic Orbital (GIAO) self consistent method using Polarizable Continuum Model (I-PCM model) at B3LYP/6–311++G (2d,p) basis set. The Mullikan charge distortion due to the chemical change of molecular orbitals was mapped and the values were purposively analyzed for the identification of key role for pharmaceutical functional process of the compound. The DM, linear polarizability and the first order hyper polarizability in different coordinates of the compound have been extracted using B3LYP method with the 6–311++G (d,p) basis set. The enhanced ECD and VCD spectral pattern were drawn and the enantiomer characteristics of the compound were studied to explore the toxicity effect of ligands.

4. Results and discussions

4.1. Structure modification analysis

The structure of present molecule was optimized and the related parameters were calculated and are depicted in Table 1 and the corresponding diagram is presented in Fig. 1. Usually, the base structure is modified with respect to the type of ligand group injected to the ring. The reception of substitutions in the base frame is pronounced by the alteration of bond length and bond angle due to the electronic configuration of atoms in different places of the ring. Once, the changes take place in the electronic arrangement that will change all the respective parametric changes in the molecule like fundamental physical properties. Simultaneously, the physico-chemical properties are altered with respect to the effect of ligand group.

Here, the CHO–NH$_2$ groups were added in the benzene ring and the molecular structure comes in to optimized form. Here, the benzene is the base in which the substitutional groups were injected and the corresponding bond length of C2–C3 and C3–C4 were found to be enlarged by 0.005Å as in Table 1. This change of bond length showed the disturbance of chemical equilibrium forces existed among the core CC. In the ligand chain, the bond length alternation took place at C12–O15 and O15–N16 as 1.437Å and 1.440Å. Due to the higher chemical force of attraction in C12–O15 than O15–N16, the first bond length decreased in first case than second. Usually, the attraction between the atoms C and O is much higher than attraction between O and N since C is more positive than N. by the consequence of stretching of bond length O–N, the asymmetrical enlargement of bond length appeared on N–H by 1.019Å. This induced the decrement of amino flavor in the chain. As indicated in Table 1, the extraordinary bond length elongation took place over the bond C3–C12 (1.505Å) due to the repulsive forces arranged due to the forces of attraction between CHO and NH$_2$ entities. This atmosphere is making reduction of chemical intensiveness of aldehyde group. Thus, reduced amino energy with enlarged carbonyl energy blended with benzene ring by injecting ligand group, the antiseptic chemical potential was produced.

4.2. Mulliken charge decomposition analysis

The mulliken partial charge distribution diagram is depicted in Fig. 2. Once the optimized structure is obtained, it is not necessary to look at the position of the nuclei (bond distances and angles) but the electronic density to be account on charge displacement as well. The molecular orbital interaction theory provides more specific and comprehensive information regarding the electronic interactions taking place in a molecule in the form of mulliken charge population distribution called patrician of electron density [8]. The Energy Partitioning is nothing but electronic structure interaction energy which relates function of ligand groups on the functional pattern of base compound [9]. Here, the mulliken charge assignment was investigated to explore the restoring chemical kinetics for manipulating drug property.

In this case, except, C3, all the core CC of the benzene ring was looking as red, the electrostatic component was appeared and this was due to the electron density pulling by the ring for electronic interaction to make sufficient potential to prepare the drug property. Even though, usually, the repulsive chemical forces arrived between C and C in the ring, due to the reconfiguration of charge density, the electrostatic interaction was observed on the bond C3–C12. This was mainly due to the charge pulling by the amino group from O and O was found to be neutral atom from which the chemical potential was exchanged between ring and amino group via O. The Pauli repulsion component was existed between core CC and O & N and it was purely by the reorientation of electron density against protonic region (nucleolus). From the electrostatic interaction and Pauli repulsion among the electronic configuration of molecule described that, the required chemical potential for the molecule to induce the drug potential from such type of successful

Table 1

Optimized geometrical parameters for *O-Benzyl Hydroxylamine*.

Geometrical parameters	Methods				
	HF	B3LYP		B3PW91	
	6-311++G (d, p)	6-31++G (d, p)	6-311++G (d, p)	6-31++G (d, p)	6-311++G (d, p)
Bond length(Å)					
C1–C2	1.385	1.393	1.393	1.393	1.390
C1–C6	1.385	1.397	1.394	1.396	1.392
C1–H7	1.075	1.086	1.084	1.086	1.085
C2–C3	1.388	1.401	1.397	1.400	1.396
C2–H8	1.076	1.085	1.085	1.087	1.084
C3–C4	1.388	1.398	1.398	1.398	1.394
C3–C12	1.507	1.509	1.505	1.501	1.504
C4–C5	1.385	1.396	1.393	1.394	1.391
C4–C9	1.076	1.087	1.085	1.087	1.086
C5–C6	1.385	1.394	1.394	1.394	1.390
C5–H10	1.075	1.086	1.084	1.086	1.085
C6–H11	1.075	1.086	1.084	1.086	1.085
C12–H13	1.085	1.099	1.095	1.094	1.098
C12–H14	1.085	1.099	1.095	1.096	1.097
C12–O15	1.406	1.429	1.437	1.444	1.420
O15–N16	1.391	1.442	1.440	1.433	1.426
N16–H17	1.001	1.021	1.019	1.022	1.018
N16–H18	1.001	1.021	1.019	1.018	1.017
N16–Cl20	3.652	3.220	3.318	3.558	3.356
H19–Cl20	1.270	1.287	1.288	1.325	1.285
Bond angle (°)					
C2–C1–C6	120.03	120.20	120.00	119.99	120.30
C2–C1–H7	119.89	119.80	119.93	119.91	119.72
C6–C1–H7	120.08	120.01	120.08	120.10	119.98
C1–C2–C3	120.72	120.53	120.70	120.54	120.47
C1–C2–H8	119.71	120.30	119.90	119.98	120.40
C3–C2–H8	119.57	119.17	119.40	119.48	119.12
C2–C3–C4	118.77	118.88	118.82	119.05	118.87
C2–C3–C12	120.67	120.41	120.59	120.29	120.85
C4–C3–C12	120.55	120.70	120.58	120.66	120.26
C3–C4–C5	120.75	120.70	120.70	120.56	120.72
C3–C4–H9	119.57	119.49	119.39	119.60	119.56
C5–C4–H9	119.67	119.81	119.91	119.84	119.72
C4–C5–C6	120.02	120.03	120.00	119.98	120.06
C4–C5–H10	119.89	119.82	119.93	119.86	119.81
C6–C5–H10	120.10	120.15	120.08	120.16	120.13
C1–C6–C5	119.70	119.66	119.78	119.89	119.58
C1–C6–H11	120.15	120.16	120.11	120.03	120.23
C5–C6–H11	120.14	120.18	120.11	120.08	120.20
C3–C12–H13	110.83	111.06	111.20	112.04	110.66
C3–C12–H14	110.68	110.67	111.24	111.47	110.37
C3–C12–O15	108.37	108.19	107.60	108.00	108.76
H13–C12–H14	108.02	107.23	108.22	108.61	107.45
H13–C12–O15	109.48	109.13	109.27	107.57	109.16
H14–C12–O15	109.46	110.56	109.28	109.03	110.43
C12–O15–N16	110.28	108.38	108.78	108.99	108.86
O15–N16–H17	105.84	103.84	104.17	104.96	104.46
O15–N16–H18	105.76	103.42	104.18	103.27	104.14
O15–N16–Cl20	180.00	144.99	128.72	56.17	153.08
H17–N16–H18	107.00	105.43	106.19	106.41	105.93
H17–N16–Cl20	74.16	100.14	102.35	50.27	94.77
H18–N16–Cl20	74.24	94.22	109.37	104.38	88.09
N16–Cl20–H19	146.23	169.68	175.21	31.83	165.38
Dihedral angle (°)					
C6–C1–C2–C3	0.05	0.39	-0.04	0.08	0.36
C6–C1–C2–H8	-179.99	179.58	-179.99	-179.91	179.47
H7–C1–C2–C3	179.89	-179.73	179.77	179.85	-179.65
H7–C1–C2–H8	-0.15	-0.54	-0.17	-0.14	-0.54
C2–C1–C6–C5	-0.04	-0.39	-0.06	-0.05	-0.43
C2–C1–C6–H11	179.82	179.82	179.82	179.85	179.91
H7–C1–C6–C5	-179.88	179.73	-179.87	-179.82	179.58
H7–C1–C6–H11	-0.02	-0.05	0.00	0.08	-0.08
C1–C2–C3–C4	-0.06	0.15	0.14	-0.05	0.27
C1–C2–C3–C12	179.10	-178.38	179.07	179.31	-178.03
H8–C2–C3–C4	179.99	-179.05	-179.92	179.94	-178.85
H8–C2–C3–C12	-0.85	2.42	-0.99	-0.70	2.85
C2–C3–C4–C5	0.05	-0.68	-0.14	-0.01	-0.82
C2–C3–C4–H9	-179.99	179.29	179.90	179.77	179.06
C12–C3–C4–C5	-179.11	177.84	-179.07	-179.36	177.48
C12–C3–C4–H9	0.85	-2.19	0.97	0.41	-2.64

Table 1 (*continued*)

| Geometrical parameters	Methods				
	HF	B3LYP		B3PW91	
	6-311++G (d, p)	6-31++G (d, p)	6-311++G (d, p)	6-31++G (d, p)	6-311++G (d, p)
C2–C3–C12–H13	30.81	71.09	30.06	36.76	81.50
C2–C3–C12–H14	150.63	-169.93	150.75	158.71	-159.69
C2–C3–C12–O15	-89.34	-48.65	-89.57	-81.53	-38.40
C4–C3–C12–H13	-150.05	-107.41	-151.03	-143.89	-96.77
C4–C3–C12–H14	-30.23	11.58	-30.34	-21.94	22.04
C4–C3–C12–O15	89.80	132.85	89.33	97.81	143.33
C3–C4–C5–C6	-0.03	0.68	0.04	0.03	0.76
C3–C4–C5–H10	-179.88	-179.84	-179.78	179.95	-179.88
H9–C4–C5–C6	-179.99	-179.29	-180.00	-179.74	-179.13
H9–C4–C5–H10	0.16	0.19	0.18	0.18	0.24
C4–C5–C6–C1	0.03	-0.14	0.06	0.00	-0.12
C4–C5–C6–H11	-179.83	179.65	-179.82	-179.90	179.54
H10–C5–C6–C1	179.88	-179.61	179.88	-179.92	-179.48
H10–C5–C6–H11	0.02	0.17	0.01	0.18	0.18
C3–C12–O15–N16	-179.91	173.38	-179.97	174.76	172.89
H13–C12–O15–N16	59.11	52.43	59.18	53.65	52.06
H14–C12–O15–N16	-59.12	-65.28	-59.06	-63.95	-65.86
C12–O15–N16–H17	123.29	119.95	124.70	112.97	119.84
C12–O15–N16–H18	-123.40	-130.14	-124.17	-135.71	-129.23
C12–O15–N16–Cl20	-82.69	-11.94	5.69	125.72	-14.38
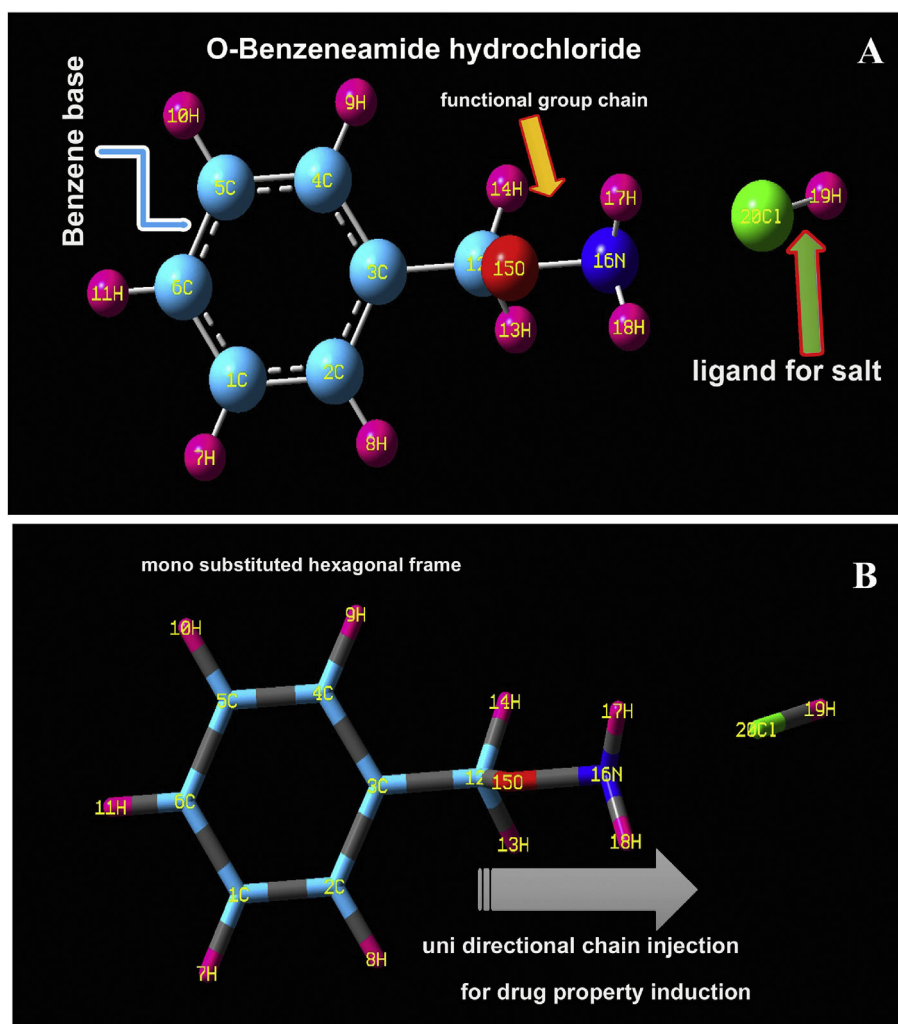
Fig. 1. (A) Bond type and (B)Tube structures of O-Benzyl Hydroxylamine.
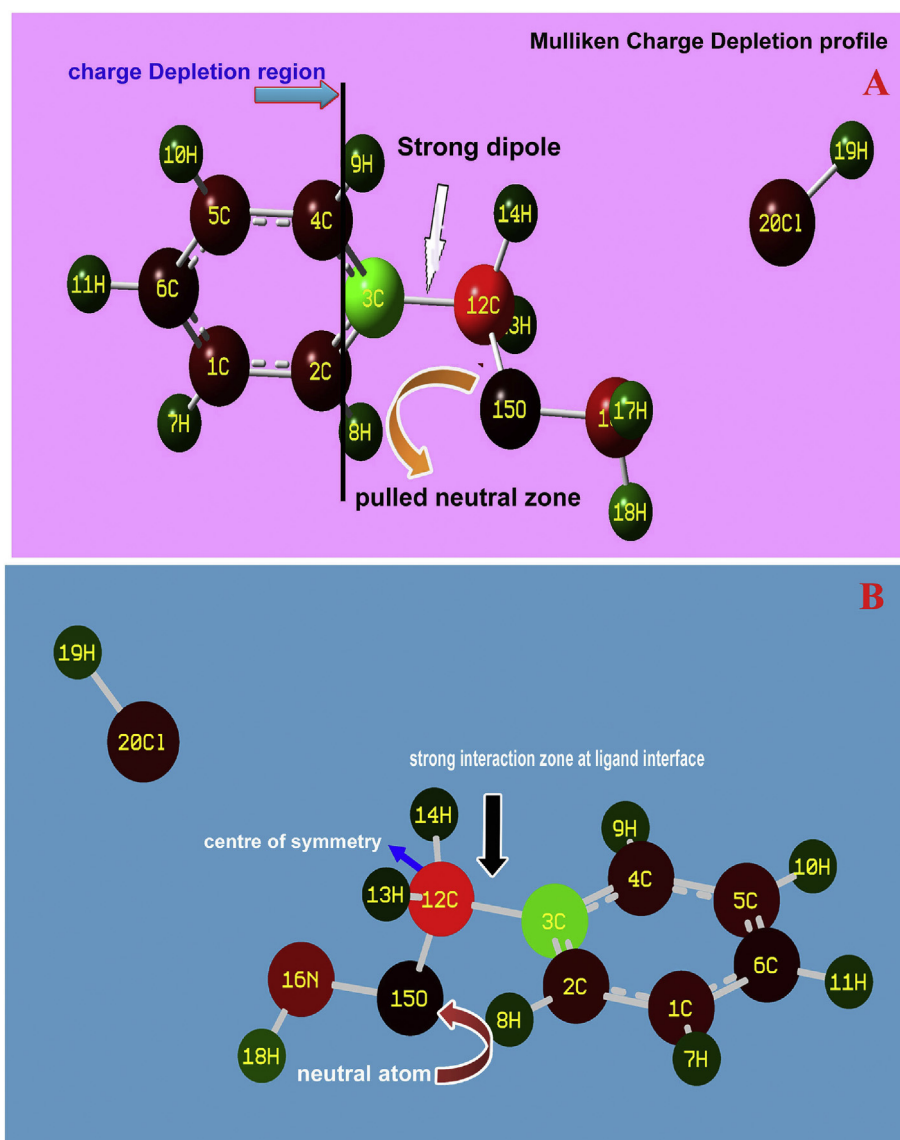
Fig. 2. (A) Plane vertical (B) plane horizontal; Mulliken charge level diagram of O-Benzyl Hydroxylamine.

electronic configuration. Here, the accepted electronic configuration in terms of mulliken charge assignment for this case elucidate that, the chemical potential which was extracted from amino group was mainly used for incrementing antiseptic kinetics in the molecule. Thereby, the antiseptic property was stimulated as in the required rate in the molecule.

The centre of symmetry point of chemical equivalent forces was papered on C12 on which the exchange of chemical potential was found to be oscillated between ring and amino group and finally, in the ground state structure (Optimized), the mulliken charge orientation favour for the inducement of drug property. The resultant drug energy gained from the fragmentation of orbitals in base and ligand groups are able to relax into an optimal form at the point of O in the molecular complex.

4.3. Biological importance investigation

The biological parameters were observed from Molinspiration program, are presented in Table 2 and the lipophilicity diagram is illustrated in Fig. 3. Usually the Molecular mono isotopic mass of the drug compound decides transport properties of molecules, such as blood-brain barrier penetration (BBB) which is most important molecular-ligand properties of drug. The drug molecules do not cross BBB in order to choose the non-CNS targets [10]. The molar Volume of this compound

Table 2
Biological parameters of *O-Benzyl Hydroxylamine*.

Parameters	values
Hydrogen bond donor count	2
Hydrogen bond acceptor count	2
Rotatable bond count	2
Topological Polar Surface Area	32.5 Å^2
Mono isotopic Mass	159.045 g/mol
Exact Mass	159.045 g/mol
Heavy Atom Count	10
Covalently-Bonded Unit Count	2
LogP	1.28
N atoms	9
MW	123.16
nON	2
nOHNH	2
volume	121.12
GPCR ligand	2.14
Ion channel modulator	1.38
Kinase inhibitor	2.28
Nuclear receptor ligand	2.35
Protease inhibitor	1.80
Enzyme inhibitor	1.19

CPK 3D view

Molecular Lipophilicity Potential

O-Benzyl Hydroxylamine Hydrochloride

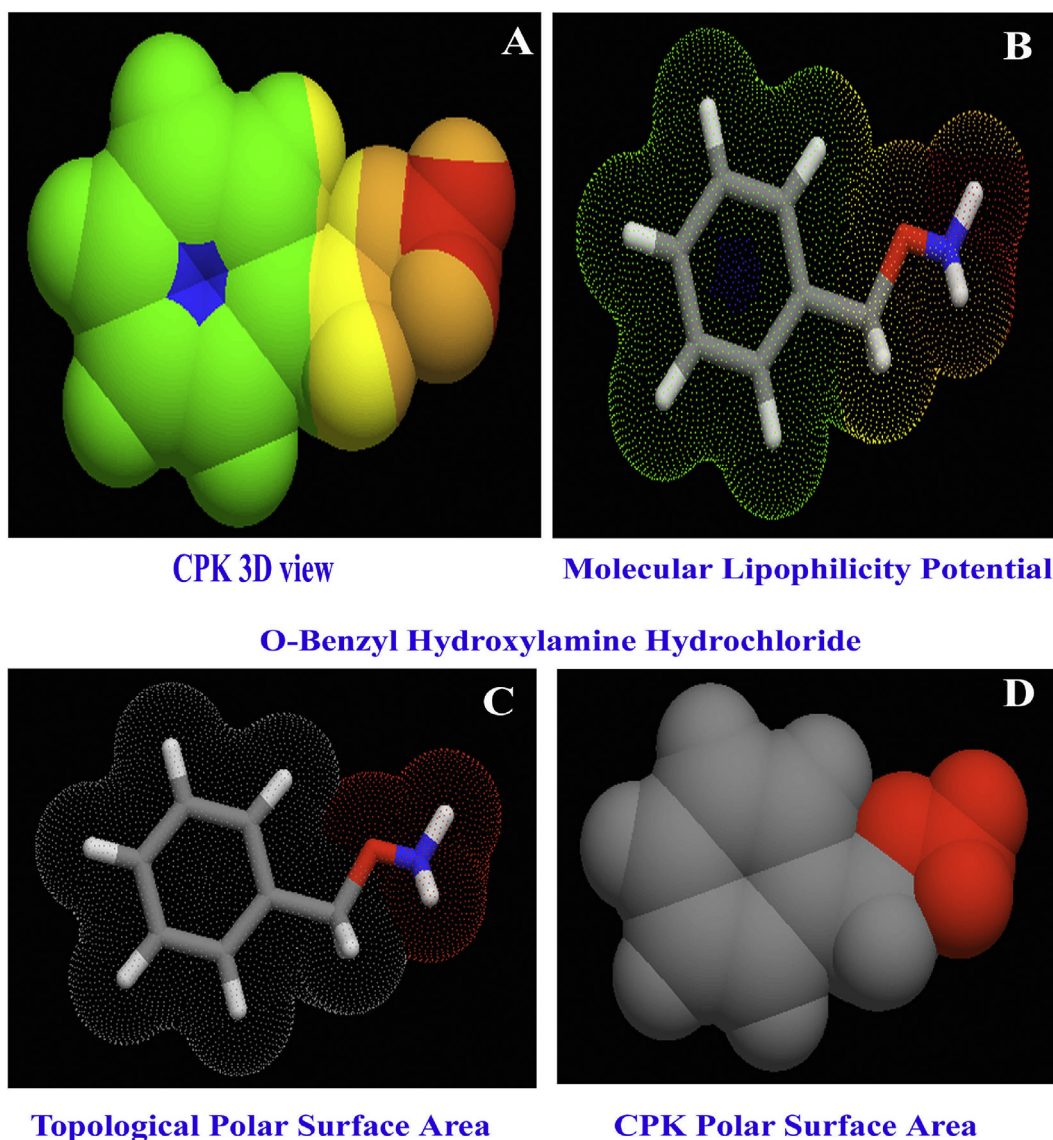**Topological Polar Surface Area**

CPK Polar Surface Area

Fig. 3. (A) CPK view, (B) MLP view, (C) TPS view and (D) PSA view of O-Benzyl Hydroxylamine.

was found to be 121.12 which is the limited coefficient that will choose the right target to avoid the side effects. The logP is nothing but Octanol-water partition coefficient and is a measure of molecular hydrophobicity which ensure the drug absorption and bioavailability of the chemical compound. Here, the logP was found to be 1.28 and was very low value. In addition to that, the present molecule able to have additive ligand groups for the improvement of the drug properties.

The topological surface area is the passive molecular transport properties of the drug molecule which enable the good transport properties for the targeting molecules [10]. For the present drug, the TPSA was determined to be 32.5 A^2 and this value is measured to be very low when compared with allowed rate and the molecule can be added with more number of ligand groups in order to stabilize the drug ability further. According to the Lipinski five rule, the Hydrogen bond donor (HBD) count, Hydrogen bond acceptor (HBA) count, Topological Polar Surface Area, logP and Rotatable bond count are to be within the expected value such as 5:5:140:10:5. For this drug case, all were determined to be 2:2:32.2:1.28:2 respectively and these parameters value was ensured to be within the allowed limit which satisfied the RO5 [11, 12].

The GPCR ligand is a 7-T integral membrane protein and sensory signal mediator protein which was found to be 2.14 for the present

compound. From the observed value, it was found that, it was optimized value that transduces extracellular stimuli into intracellular signals usefully. The ion channel modulator is pore like membrane protein which permit ion to pass via the channel pore which transduce the signal to generate the action potential across the cell membrane. For the present case, it was calculated to be 1.38, is enough to modulate the signal proportionate to the drug action. Kinase inhibitor is the drug substance that blocks a kind of enzyme called kinase that controls the function the cell signaling and metabolism. The present case is already antiseptic compound and has the calculated value of kinase inhibitor been 2.28 which are enough to inhibit the action of the blood vessels to help the unusual growth of cells. The nuclear receptor is the protein that has ability to directly interact with DNA and control the expression of genomic DNA. Here, the related value of the same was determined to be 2.35 which is trace value of the expected limit. So the present molecule has the ability to interact with corresponding protein and isolate the function of organ. The Protease and enzyme inhibitor coefficient were found to be 1.80 and 1.19 respectively. Here, these values are moderate and both the inhibitors are ligand-molecules which can hold back the function of proteases and enzymes which were supported by the literature [13].

4.4. Vibrational analysis

4.4.1. Vibrational assignments

The optimized molecular structure was composed by 18 atoms in terms of base and ligand groups. In order to study the vibrational characteristics, the IR and Raman peaks are to be assigned to compositional bonds on the vibrational pattern and the respective values along with calculated values are depicted in Table 3. The assigned frequencies with respect to fundamental and group frequency rules for cyclic compound (Vib. = 3n-6). The in plane and out of plane vibrations of compositional bonds are classified and represented by $\overset{\approx}{\mu}$ and $\overset{\sim}{\mu}$. According to the mutual exclusion principle [14], the total number of vibrations was found to be 48 in which 18 stretching, 15 in plane bending and 15 out of plane bending were assigned and their related FT-IR and FT-Raman spectral pattern are displayed in Figs. 4 and 5 respectively.

$\Gamma vib = 33\ \mu' + 15\ \mu''$

4.4.2. C–H vibrational pattern

The base of O-Benzyl Hydroxylamine was benzene in which apart from the substitutional place, it contains five C–H bonds. Due to the ligand insertion, the characteristics vibrations of the same may be affected. Actually, for the benzene and its derivatives, the C–H stretching, in plane bending and out of plane bending modes can be assigned in the region of 3080–3010 cm^{-1}, 1290-990 cm^{-1} and 980-750 cm^{-1} correspondingly [15, 16]. In present vibrational pattern, the C–H stretching, in plane and out of plane bending vibrational bands were identified at 3030, 3020, 3010, 3005 and 2980 cm^{-1}, 1180, 1175, 1160, 1100 and 1050 cm^{-1} and 995, 985, 970, 930 and 880 cm^{-1} respectively. Except some vibrational bands, the stretching bands were clearly appeared to be moved down to well below the expected limit and the in plane bending modes were restricted within the expected limit whereas the out of plane bending signals have been observed at the top end of the allowed region.

Table 3
Experimental and calculated vibrational frequencies *O-Benzyl Hydroxylamine*.

Symmetry species C_s	Observed frequency (cm^{-1})		Methods					Vibrational assignments
			HF	B3LYP		B3PW91		
	FT-IR	FT-Raman	6-311++G (d, p)	6-31+G (d, p)	6-311++G (d, p)	6-31+G (d,p)	6-311++G (d, p)	
μ'	3450m	-	3455	3440	3439	3442	3455	(N–H) υ
μ'	-	3350vw	3355	3351	3359	3335	3343	(N–H) υ
μ'	-	3030vw	3028	3029	3044	3033	3033	(C–H) υ
μ'	-	3020vw	3019	3022	3009	3023	3025	(C–H) υ
μ'	-	3010vw	3010	3012	3000	3015	3013	(C–H) υ
μ'	-	3005vw	2973	2974	2992	2976	2971	(C–H) υ
μ'	2980vs	-	2997	2996	3015	3003	2995	(C–H) υ
μ'	-	2900vw	2914	2913	2893	2904	2909	(C–H) υ
μ'	2880vs	-	2878	2879	2879	2877	2874	(C–H) υ
μ'	1610m	1610w	1651	1654	1640	2850	1609	(C=C)υ
μ'	1605m	1605vw	1608	1602	1608	1647	1605	(C=C)υ
μ'	1590s	-	1597	1588	1587	1607	1587	(C=C)υ
μ'	-	1480vw	1481	1476	1479	1590	1481	(C–C) υ
μ'	-	1470vw	1479	1476	1470	1484	1470	(C–C) υ
μ'	1450m	-	1446	1445	1449	1473	1448	(C–C) υ
μ'	1400m	-	1401	1400	1431	1450	1394	(C–C) υ
μ'	1330vw	-	1328	1329	1333	1408	1326	(C–O–N) υ
μ'	-	1320vw	1317	1323	1320	1334	1315	(C–O) υ
μ'	1230vw	-	1227	1240	1237	1316	1230	(N–H) δ
μ'	-	1220w	1217	1222	1213	1294	1223	(N–H) δ
μ'	1180w	-	1183	1180	1176	1224	1180	(C–H) δ
μ'	-	1175vw	1182	1175	1174	1180	1173	(C–H) δ
μ'	1160m	-	1163	1166	1162	1174	1158	(C–H) δ
μ'	-	1100vw	1102	1100	1104	1163	1103	(C–H) δ
μ'	-	1050vw	1054	1052	1050	1100	1049	(C–H) δ
μ'	1030vw	-	1034	1036	1031	1050	1029	(C–H) δ
μ'	1010vs	-	1013	1010	1013	1028	1007	(C–H) δ
μ'	1005vs	-	1001	1005	1023	1010	1006	(N–H) γ
μ'	-	1000vs	1003	1004	1018	1008	999	(N–H) γ
μ'	-	995vs	990	1000	1012	1006	997	(C–H) γ
μ'	985w	-	981	988	1005	1000	995	(C–H) γ
μ'	-	970vw	967	944	958	991	970	(C–H) γ
μ'	930w	-	930	924	936	959	931	(C–H) γ
μ'	880s	-	880	864	875	933	870	(C–H) γ
μ'	-	820vw	821	820	822	864	819	(C–H) γ
μ'	750vs	-	753	750	751	818	759	(C–H) γ
μ'	700vs	-	700	701	697	749	702	(C–O) δ
μ'	610m	-	608	612	607	703	611	(C–O–N) δ
μ'	600vw	-	599	601	599	610	603	(CCC) δ
μ'	-	500vw	500	500	501	599	494	(CCC) δ
μ'	410vw	-	409	410	411	501	410	(CCC) δ
μ'	-	350vw	351	350	351	410	350	(C–O) γ
μ''	-	300vw	300	300	300	350	300	(C–O–N)γ
μ''	-	290vw	290	290	289	300	284	(C–C) δ
μ''	-	180w	180	179	180	290	181	(CCC) γ
μ''	-	140m	139	141	140	180	140	(CCC) γ
μ''	-	120vs	120	120	120	140	120	(CCC) γ
μ''	-	105s	105	105	105	120	105	(C–C) γ

VS –Very strong; S – Strong; m- Medium; w – weak; as- Asymmetric; s – symmetric; υ – stretching.
α –deformation, δ - In plane bending; γ-out plane bending; τ – Twisting.
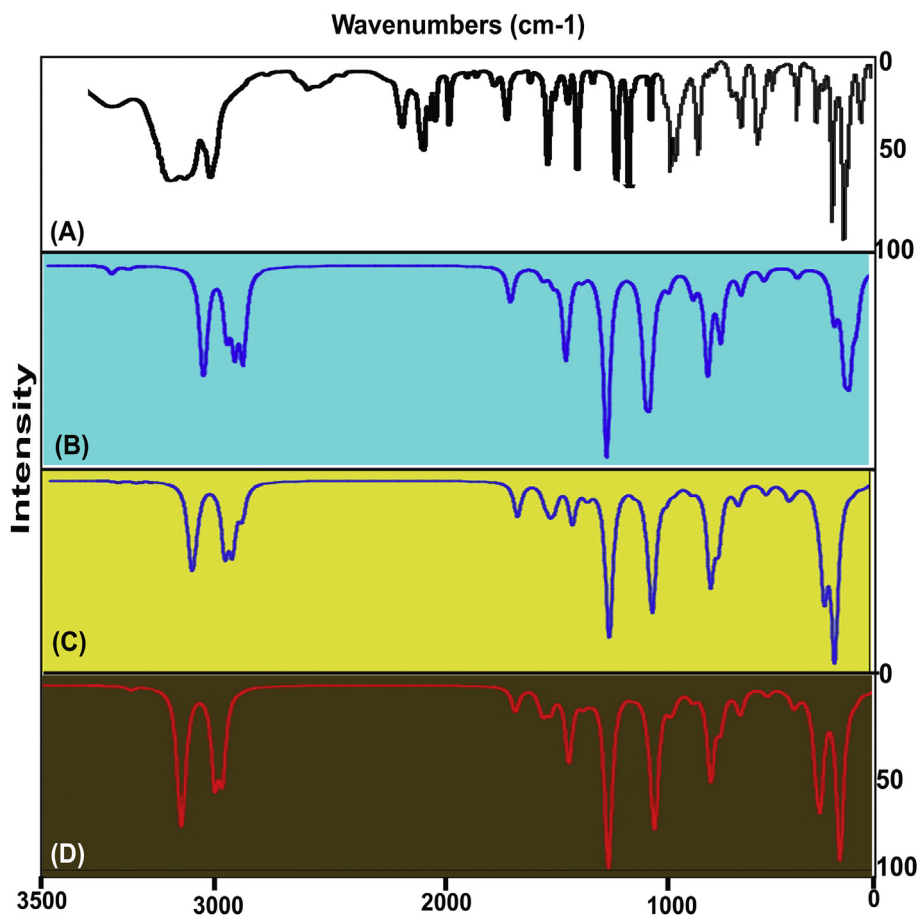
Wavenumbers (cm-1)

Fig. 4. (A) Experimental and Calculated (B) HF, (C) B3LYP, (D) B3PW91 FT-IR spectra of O-Benzyl Hydroxylamine.

Such observed view showed that, some of the vibrational energy related to the chemical potential was consumed by the substitutional groups. So that, equivalent chemical potential of the ring was altered with respect to the ligand groups and the chemical property was definitely rehabilitated in to the chemical assistance provided by the ligand groups. Here, in such a way, the antiseptic property of the present compound was found to be prepared by the ligand potential blended with benzene ring.

4.4.3. Core ring vibrations

The aromatic ring core vibrations called CC stretching, in plane and out of plane ring breathing modes for benzene and its derivative chemical species are observed in the region 1600-1430 cm^{-1}, 630-605 cm^{-1} and 560-415 cm^{-1} respectively [17, 18, 19]. The present case was mono substituted benzene derivative and the respected CC stretching bands were identified at 1610, 1605 & 1590(C=C) cm^{-1}, 1480, 1470 & 1450 (C–C) cm^{-1} as in Table 3. The in plane and out of plane ring breathing vibrational modes have been observed in the IR and Raman spectra at 600, 500 & 410 cm^{-1} and 180, 140 & 120 cm^{-1} respectively. Since the core CC stretching bands were found at top end of the expected limit, there was no chemical energy related to such vibrations taken by the substitutional groups. Instead of that, the ring breathing modes have been observed to be suppressed much due to chemical energy suction by the taken up ligand groups. Only low order bond energy was absorbed by the substitutional groups and thereby that energy was consumed for blending of property of benzene and ligand groups.

4.4.4. Amino group and ethyl group vibrations

The amino group in the base compound always dominates the vibrational characteristics as well as chemical property organizer. If it is substituted directly, it will be dominated straight and affect the

molecular property rationally. If it is substituted along with the passive and active substitutional groups, it will inject the bound ligand property into the base compound. So, the methoxy enthalpy energy is transferred to the ring by amino group via ethyl group. Since the energy transferred from amino group, the chemical energy may be affected little bit. As per Table 3, vibrations of N–H group was found to be 3450 and 3350 cm^{-1} (stretching), 1230 & 1220 cm^{-1} (in plane bending) and 1005 & 1000 cm^{-1} (out of plane bending) respectively to pronounce the amino group in the ring. Generally, in the case of hydroxylamine, the stretching, in plane and ut of plane bending vibrational bands are assigned in the region 3255-3235 cm^{-1}, 1450-1200 cm^{-1} and 895-650 cm^{-1} respectively [20]. Actually, instead of suppression of vibrational energy of amino group due to the conjugation of methoxy group, the vibrational bands have elevated to the higher vibrational region when compared with expected limit. The dominated character and endothermic property of the amino group was proved in this case also.

4.4.5. C–O–N and C–O vibrations

The hydroxylamine compound has finite wavenumber in the region 855-840 cm^{-1} for C–O–N stretching band, 510-420 cm^{-1} for C–O–N in plane bending and below 300 cm^{-1} for C–O–N out of plane bending modes. In this case, the stretching, in plane and out of plane bending modes were observed at 1330, 610 and 300 cm^{-1} correspondingly for the methoxylamine group. From this vibrational process, it was traced that, the bridge bond of C–O–N was intensively pronounced in the wavenumber assignment for the present compound. The C–O stretching signals are normally denoted around the region 1050 cm^{-1} whereas in this case, it was observed at 1320 cm^{-1} and the in plane and out of plane bending bands were recognized at 700 and 350 cm^{-1} respectively. All the vibrational enthalpy energy in the chain bonds were found to be active
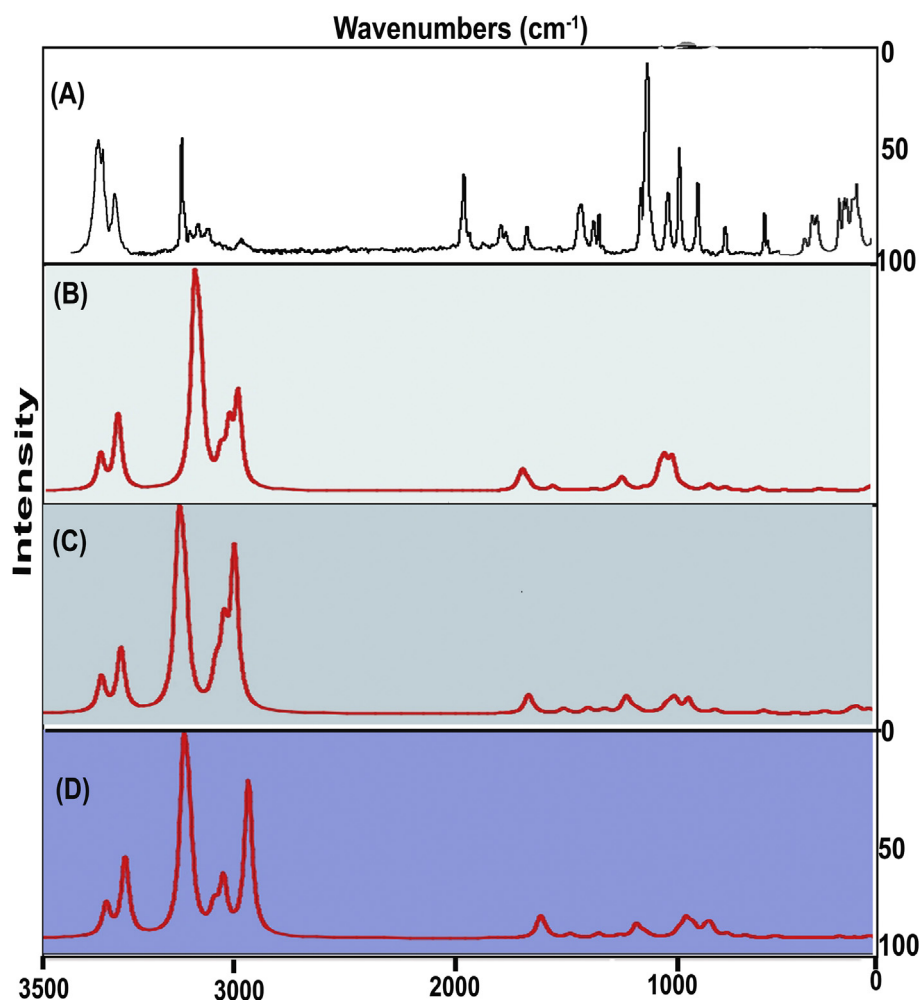
Fig. 5. (A) Experimental and Calculated (B) HF, (C) B3LYP, (D) B3PW91 FT-Raman spectra of O-Benzyl Hydroxylamine.

and energized to send the chemical energy to the chain to provide the specific drug kinetics.

4.5. NMR chemical interpretation

The chemical reactivity mechanism of the chemical compound is formulated with respect to the chemical shift regulated in the core as well as ligand merged carbons and their related hydrogens [21]. Usually, the chemical reaction path can be identified through the core carbons due to the charge dislocation take place around the ligand groups are added to the appropriate places in the compound [22]. The chemical mechanism for generating the useful drug activity in the chemical species is setup by the adopting atoms or molecules with the base compound. The charge domain displacement from atom to atom in the molecular entities is achieved by chemical equivalent molecular kinetic forces in the form of coagulation of diamagnetic shield breaking which leading asymmetric charge gradient. The NMR chemical shift representation was presented in Table 4 and its graphical spectra are depicted in Fig. 6.

In this case, this was observed as usual that, the core carbon C3 has shifted more than other carbons in the ring which was the substitutional place. But, the chemical shift core carbons C5, C6 and C1 have unusually shifted (Cal. = 133, 132 and 134 ppm) (Expt. = 128, 127 and 134 ppm). This view showed the extension of reaction path in the core carbons and abruptly the same chemical environment was observed. In the case of C2 and C4, the chemical shift (Cal. = 130 ppm) was found to be lower than C1, C5 and C6, and from which the nodal point of core carbons were identified. This impact was felt in the uniform chemical shift of allied
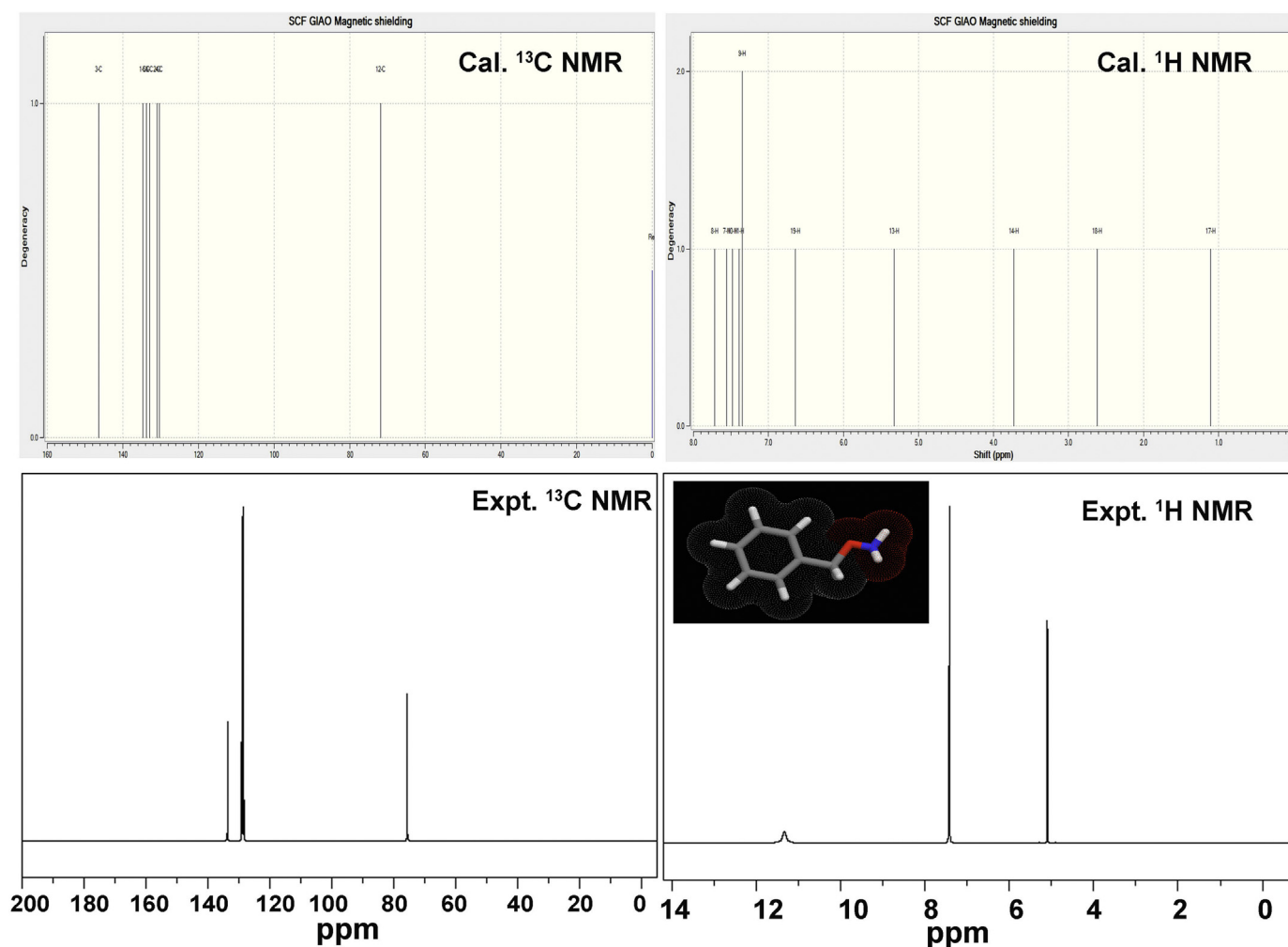
Table 4
Experimental and calculated ^{1}H and[13]C NMR chemical shift in *O-Benzyl Hydroxylamine.*

Atom position	Chemical shift - TMS-B3LYP/6-311+G (2d,p) (ppm)			Experimental shift (ppm)
	Gas	Solvent phase		
		DMSO	CCl$_4$	
C1	134.25	134.62	134.65	134.0
C2	131.92	130.95	131.61	127.0
C3	145.25	146.28	145.69	135.0
C4	129.21	130.33	129.60	126.5
C5	133.08	133.77	133.30	128.0
C6	132.78	132.91	132.80	127.5
C12	71.87	71.87	71.86	75.0
H7	7.424	7.558	7.480	7.30
H8	7.723	7.714	7.727	7.35
H9	7.101	7.351	7.195	7.3
H10	7.298	7.479	7.368	7.3
H11	7.242	7.392	7.301	7.3
H13	5.426	5.325	5.395	5.15
H14	5.426	5.325	3.549	5.10
H17	2.105	2.256	2.537	-
H18	2.073	2.615	2.294	-
H19	6.534	6.641	6.568	-

Fig. 6. (A) ^{13}C, (B) ^{1}H Experimental and (C) ^{1}H, (D) ^{13}C Calculated NMR spectra of O-Benzyl Hydroxylamine.

hydrogens; H7, H9, H10 and H11 (ranged from 7.1 ppm to 7.7 ppm). From this chemical shift of core carbons, it was clear that, the acquired or oriented resultant chemical potential from the chain was restored over the carbons which were identified as chemical shift.

The chemical shift of nodal point carbon; C12 was found to be 71(Cal.) and 75 (Expt.) ppm for ligand chain. This is very low and was due to the refilling of electron domain at the breaking shield of carbonC12 which was gained from the O–NH$_2$ group. The C12 was ensured to be oscillating nodal point about which the chemical potential is oscillated back and forth to facilitate the antiseptic drug potential. Simultaneously, endothermic enthalpy energy was transited from the amino group which was accumulated in O. As the partial charge domain favor for regulating reaction path to charge chemical flavor, the desired chemical potential was attained in the molecular site.

4.6. Molecular interaction profile

The bonding MOs primarily hold base as well as ligand character to interact with each other and the degenerative orbitals communicated in terms of chemical energy accumulated in the form of nucleophilic and electrophilic to explain the structure and reactivity of molecules [23]. The molecular reactivity for the formation of useful application is represented by sensitive types of bonding and is shown in Fig. 7 and the energy levels shown in Table 5. Accordingly, the δ-nucleophilic bonding interaction (HOMO) appeared on the semicircle of the benzene ring which is isolated from the ligand group and small ligand interactive

overlapping was found on the ligand group separately. Here, two discrete orbital interactions take place for generating individual chemical characteristics and they found to be ready to donate the electron domain for enabling reactivity. In first order electrophilic orbital interaction (LUMO) called unfilled interfacial space orbital system. Here, the σ-bonding overlapping was found and among them, the diagonal cross interaction was appeared. One of the σ-bond of core carbon was interlinked with C12 of ligand group which is able to blend the obtained electron cloud character with benzene ring. In the case of HOMO, the interconnected bond orbitals opened to nucleophilic interaction in which the degenerate orbitals overlapped with one another and making group interaction domain cloud. In the case of LUMO, the σ-interactive orbitals overlapped with one another formed electrophilic affinity orbital array by which the electronic domain with restricted chemical energy of 2.95 eV can be established.

In second order nucleophilic interactive orbitals, π-bond interactive zones were found in semicircle of benzene ring and which are appeared to be interlinked with degenerate orbitals of CH$_2$O and NH$_2$. Here, the space interaction orbital lobe was seen in H with N and it was shown in Figure. In the second order LUMO orbital interaction, there was no electrophilic zone observed to enhance the remaining molecular property. In this case, all the property making process was occurred in first order only and it was clearly showed the molecular direct drug property. From this observation, it was inferred that, this molecule is able to have additional ligand group for preservative drug potential.
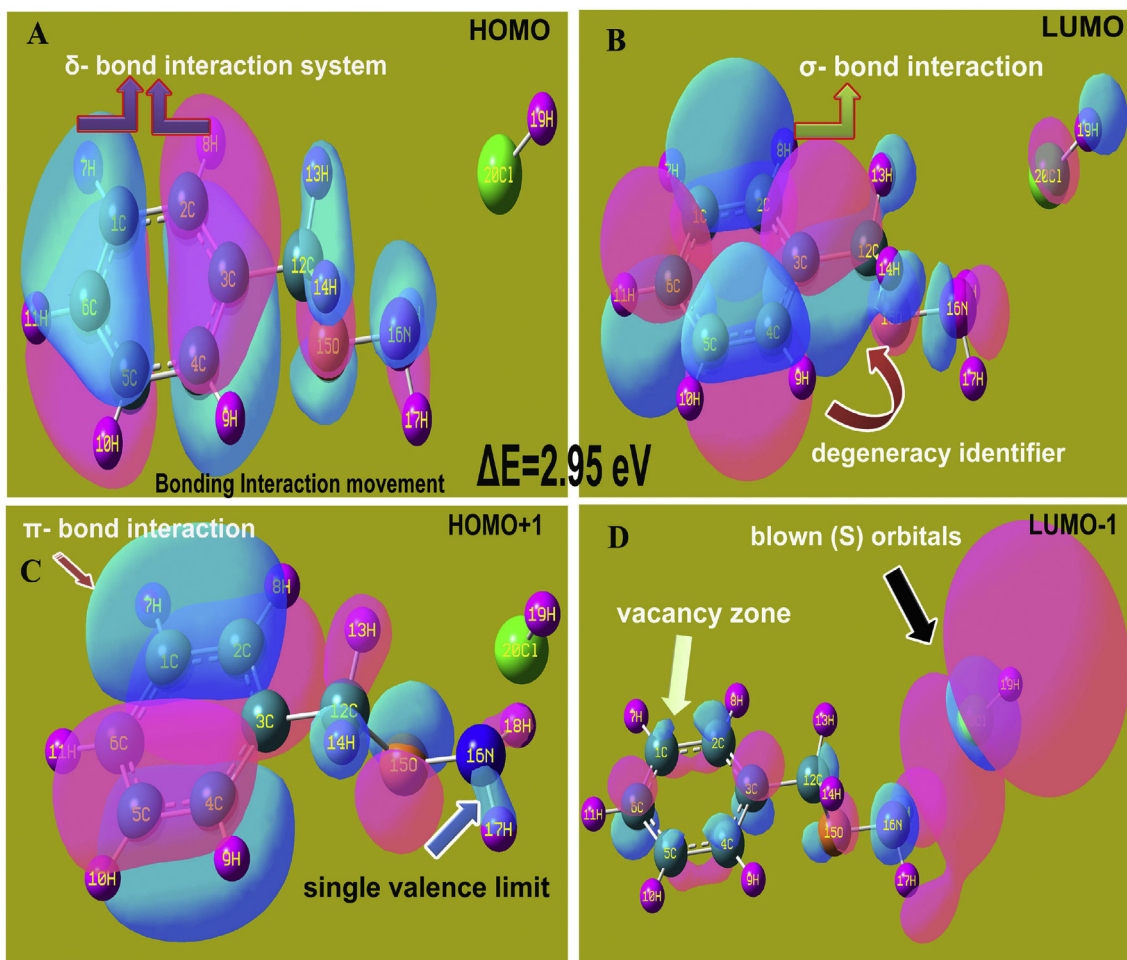
Fig. 7. (A) HOMO, (B) LUMO, (C) HOMO+1 and (D) LUMO-1; Frontier molecular interaction view of O-Benzyl Hydroxylamine.

Table 5
Frontier molecular orbitals with energy levels of *O-Benzyl Hydroxylamine*.

Energy levels	IR region	UV-Visible region
	B3LYP/6311++G (d,p) Energy (eV)	B3LYP/6311++G (d,p) Energy (eV)
H+10	11.129	11.607
H+9	10.674	11.189
H+8	10.039	10.248
H+7	9.4541	10.057
H+6	9.3566	9.647
H+5	8.9487	9.565
H+4	8.9436	8.683
H+3	7.4554	8.345
H+2	7.2717	7.105
H+1	7.0006	6.953
H	6.9811	3.760
L	0.6348	0.802
L-1	0.5962	0.610
L-2	0.4272	0.566
L-3	0.1257	0.145
L-4	0.0329	0.097
L-5	0.2754	0.231
L-6	0.4740	0.485
L-7	0.7818	0.562
L-8	0.9372	0.770
L-9	1.2865	1.016
L-10	1.3105	1.160

4.7. UV-visible spectra-CT complex

Usually, the UV-Visible spectra represented the electronic absorption process take place inside the electronic configuration of molecular system [24]. UV-Visible joint spectral pattern clearly showed the vibrational energy exchange between the molecular entities via bonds made from the incorporation of base and ligand groups [25]. By the accumulated electronic transitions in the form of absorptive peak in the respective electronic region of spectrum, the formation of CT complex in the molecular system is viewed. Though, there are many background causes to describe the formation of CT complex and it is very difficult to explain the CT mechanism structure [26].

Here, the CT complex spectral peak was observed at 590 nm along with supplementary peaks at470 and 480 nm as shown in Fig. 8. The calculated spectral values are depicted in Table 6 and according to which the peaks at 609, 484 and 473 (Cal.) at oscillator strength of 0.04, 0.005 and 0.01 with the energy gap of 2.03, 2.55 and 2.62 eV respectively. These absorption peaks were assigned to n-π* transition which belongs to R-Band (German, radikalartig) and especially, these electronic signals situated at higher wavelength region (Visible–red region). If the electronic spectral peak is observed at visible region for the chemical species and it will be very active with visible light (Photo catalytic excitation). Here, the entire spectral pattern appeared in visible red and blue regions which showed that, the present chemical is photo-active and produce photo-catalytic process in chemical reaction. All the transitional modes were displayed in spectrum by obtaining the chemical energy from HOMO to LUMO-1 and second order orbital sequence. Here, from the
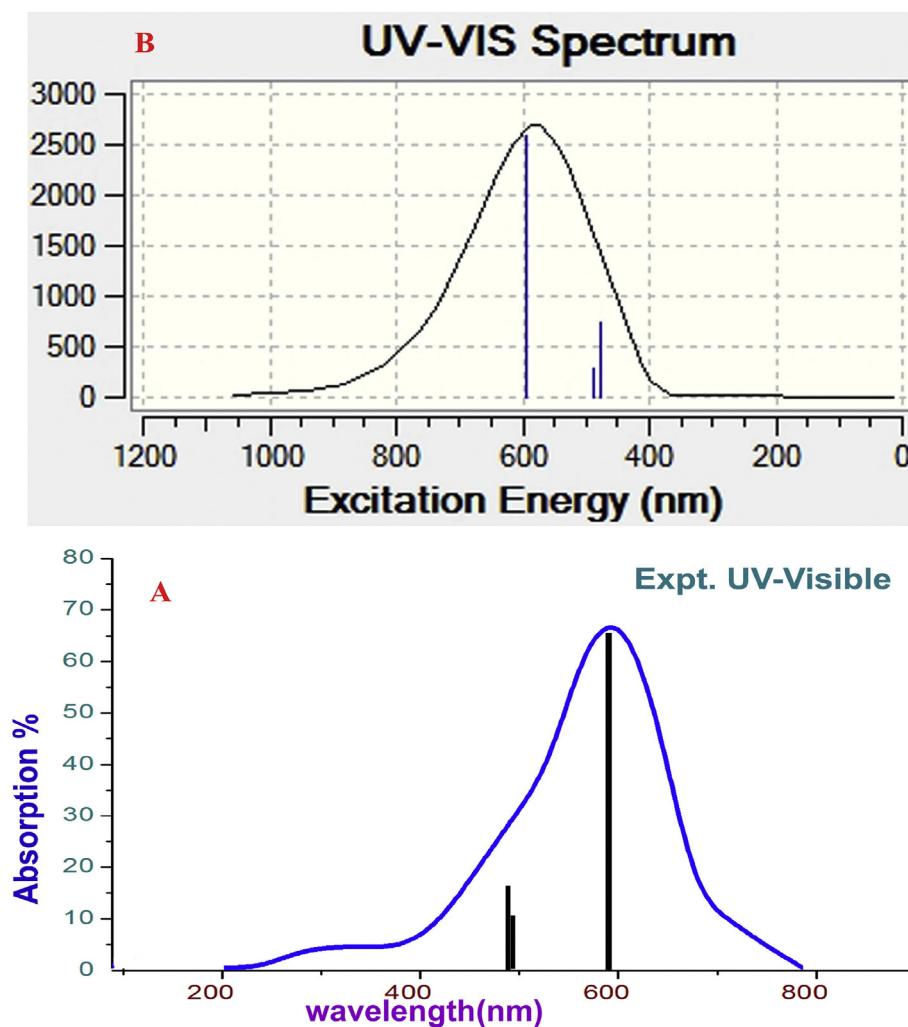
Fig. 8. (A) Experimental and (B) Calculated UV-Visible spectra of O-Benzyl Hydroxylamine.

Table 6
Theoretical electronic absorption spectral values of *O-Benzyl Hydroxylamine*.

λ (nm)	E (eV)	(f)	Transition level	Major contribution	Assignment	Region	Bands
Gas							
609.47	2.0343	0.0488	H→L (69%)	H→L	n→π*	Visible-red	R-band (German, radikalartig)
484.67	2.5581	0.0052	H→L-2 (58%)	H→L-1		Visible-blue	
473.03	2.6210	0.0159	H→L-1 (59%)	H+1→L		Visible-blue	
DMSO							
556.25	2.2289	0.0588	H→L (53%)	H→L	n→π*	Visible-blue	R-band (German, radikalartig)
488.11	2.5401	0.0154	H→L-2 (42%)	H→L-1		Visible-blue	
484.01	2.5616	0.0140	H→L-1 (62%)	H+1→L		Visible-blue	
CCl₄							
594.42	2.0858	0.0604	H→L (64%)	H→L	n→π*	Visible	R-band (German, radikalartig)
486.80	2.5469	0.0068	H→L-2 (57%)	H→L-1		Visible-blue	
478.37	2.5918	0.0173	H→L-1 (61%)	H+1→L		Visible-blue	

H: HOMO; L: LUMO.

nucleophilic and electrophilic interaction arrangement and electronic absorption peaks showed that, the C–C and O–N were found to be CT complex by which the antiseptic as well as antibiotic properties in the compound was induced.

4.8. Physico-chemical parameters

For the optimized structure, the molecule should have very low vibrational energy at zero state. Here, the molecular structure without cis and trans formation, has the zero point vibrational energy of 863 and 862 Hartree in IR and UV-Visible region respectively. So it was concluded that, the structure was comfortably making fundamental property with low amount of energy in UV-Visible region than IR. The resultant dipole moment of the molecule was 1.18 and 2.09 dyne in both regions respectively. This was comparatively low which is due to the molecule situated in restricted planes and occupies very low 3D space view. All the physico-chemical parameters are illustrated in Table 7.

The electron affinity and ionization potential were 6.9 & 3.7 and 0.63

Table 7
Physico-chemical parameters of *O-Benzyl Hydroxylamine*.

Parameter	IR region	UV region	Electrophilicity charge transfer (E_{CT}) $(\Delta N_{max})_{A^-}$ $(\Delta N_{max})_B$
E_{total} (Hartree)	-863.02	-862.76	
E_{HOMO} (eV)	6.981	3.760	
E_{LUMO} (eV)	0.634	0.801	
$\Delta E_{HOMO\text{-}LUMO\ gap}$ (eV)	6.346	2.958	
E_{HOMO+1} (eV)	7.000	6.953	+2.226
E_{LUMO-1} (eV)	0.596	0.610	
$\Delta E_{HOMO\text{-}1\text{-}LUMO+1\ gap}$ (eV)	6.404	6.342	
Chemical hardness (η)	3.173	1.479	
Electronegativity (χ)	3.807	4.562	
Chemical potential (μ)	6.346	2.958	
Chemical softness(ξ)	0.131	0.338	
Electrophilicity index (ψ)	2.284	7.035	
Dipole moment	1.189	2.099	
E_{CT}	2.454	-2.910	

& 0.80 respectively in both regions. The electron affinity was more in IR than UV-Visible region which was by the vibrational energy levels are more than electronic energy levels. So, the vibrational characteristics were better than electronic properties. The chemical energy band gap in IR region (6.34 eV) was found to be higher than UV-Visible region (2.95 eV). Here, the molecule was highly stable in IR than UV and it was more feasible in UV than IR. The chemical hardness and softness are calculated to be 3.17& 1.47 and 0.13 & 0.33 IR and UV regions respectively. Here, the chemical inertness was so high and compliance was so poor and the present compound is able to receive more ligand groups to explore different physico-chemical properties. The chemical potential of the present case was measured to be 6.34 and 2.95 in IR and UV regions. In IR since the vibrational as well as structural characteristics were stabilized more than UV region. The aromatic species are always structurally as well as chemically very weak in UV-Visible region because the electronic configuration is not stable in that region. Here, the UV-Visible activity of the present case also weak and chemically not stable.

The Electronegativity (χ) of the present case found to be 3.80 and 4.56 in respective regions which were so high in both regions. The resultant electronic properties were slightly lower in IR region than UV-Visible region since the electron cloud orientation was exposed intensively. The Electrophilicity index (ψ) was determined to be 2.28 and 7.02 respectively in both regions and it was huge in UV region due to the instant oscillation of charge configuration. The Electrophilicity charge transfer of the present case was measured to be +2.226 which clearly explicit the chemical potential transformation from ligand to ring for generating antiseptic drug activity.

4.9. Molecular static potential view

The electrostatic potential is normally measured in terms of colour gradient scalar potential which is displayed by the depletion of protonic and electronic zones around the molecule. The molecular isosurface spreading the field around the molecule for explaining space charge radiation zones in which the source of potential can be clearly viewed [27]. Here, Fig. 9 showed the electrostatic isosurface distribution of potential. Here, the protonic region was appeared over the hydrogen bonding with N called amino group which showed higher protonic content of the molecule than other identities. Similarly, the electronic region was found to be focussed over O due to the charge pulled from C and N symmetrically. Another protonic zone was observed at H–Cl bond in the molecule which is highly protonized by pulling of electron cloud by Cl atom.

All other hydrogen zone was seen to be protonic content boundary which protect charge depletion uniformly and stabilize the charge gradient. Here, the isosurface charge distribution lobe was observed at H9 and H10 of ring, O of chain and NH of amino group. These three

sources of charge distribution acted as main source of chemical potential and causing drug activity.

4.10. Hyperactive biological activity

The molecular bonds arrangements inside the limited iso volume of the molecule produced the hyper polarization which causing the molecular components depletion multipole moments [28]. The hyperactive parameters are presented in Table 8. The active bond polarization atmosphere produced net molecular moments from which net and average polarizability were measured and are to be 144×10^{-33}esu and 194×10^{-33}esu respectively. These were extracted from intensive dipole bonds and these values so high to produce sensitive biological activity. In addition to that, the hyper active polarization also produced in the molecular site which showed the enhancement of biological involvement of the molecule. Here, it was calculated to be 294.21×10^{-33}esu and this was achieved from the resultant dipole moment of the molecule. It was considerably strong and the definite biological support can be provided by the present compound.

4.11. NBMO electronic transition analysis

According to Huckel's Molecular Orbital Theory, some of higher the non bonding molecular orbitals are filled with paired electrons (donor) and low level non bonding MO was completely unfilled (Acceptor) and according to the LCO arrangements, the interaction was induced by equilibrium interactive forces enhanced among the molecular sites [29]. Among the interactive filled and unfilled orbitals, the important chemical energy exchanged to oscillate the chemical potential to generate the source of chemical properties [30]. The energy exchange transition of title molecule is depicted in Table 9.

In this case, the interaction was found to be taking place between ring and ring and ligand groups and these exchanges of energy was very high when compared with bonding system. The important transition was observed from C1 – C6 to C2 – C3 and C4 – C5 by intake of energy of 20.35 and 19.77 kcal/mol. in terms of π-π* and σ-σ* interactive system within the ring. Similarly, the significant exchange of energy of 20.64 and 20.58 kcal/mol were identified from C2 – C3 to C1 – C6 and C4 – C5 respectively and these transitions were assigned to π-π*.

In the reversible interaction of non bonding, the same transition was found between C4 – C5 and C1 – C 6 & C2–C3 in the ring itself. For that transitional exchange of chemical potential, 20.78 and 20.61 kcal/mol. amount of energy was transferred between the non bonding orbitals of bonding species. From the lone pair of O15 the considerable amount of chemical energy was exchanged to C12–H13 and C12–H14 by taking the energy of 5.52 and 5.48 kcal/mol. which was assigned by L-σ* interactive system. Here, the moderate number of transitions was taken place by which the substantial amount of energy was exchanged in another phase to arrange the antiseptic potential. In addition to that, according to the

Table 8
The Polarizability α(a.u.) and the first Hyperpolarizability β(esu) of *O-Benzyl Hydroxylamine*.

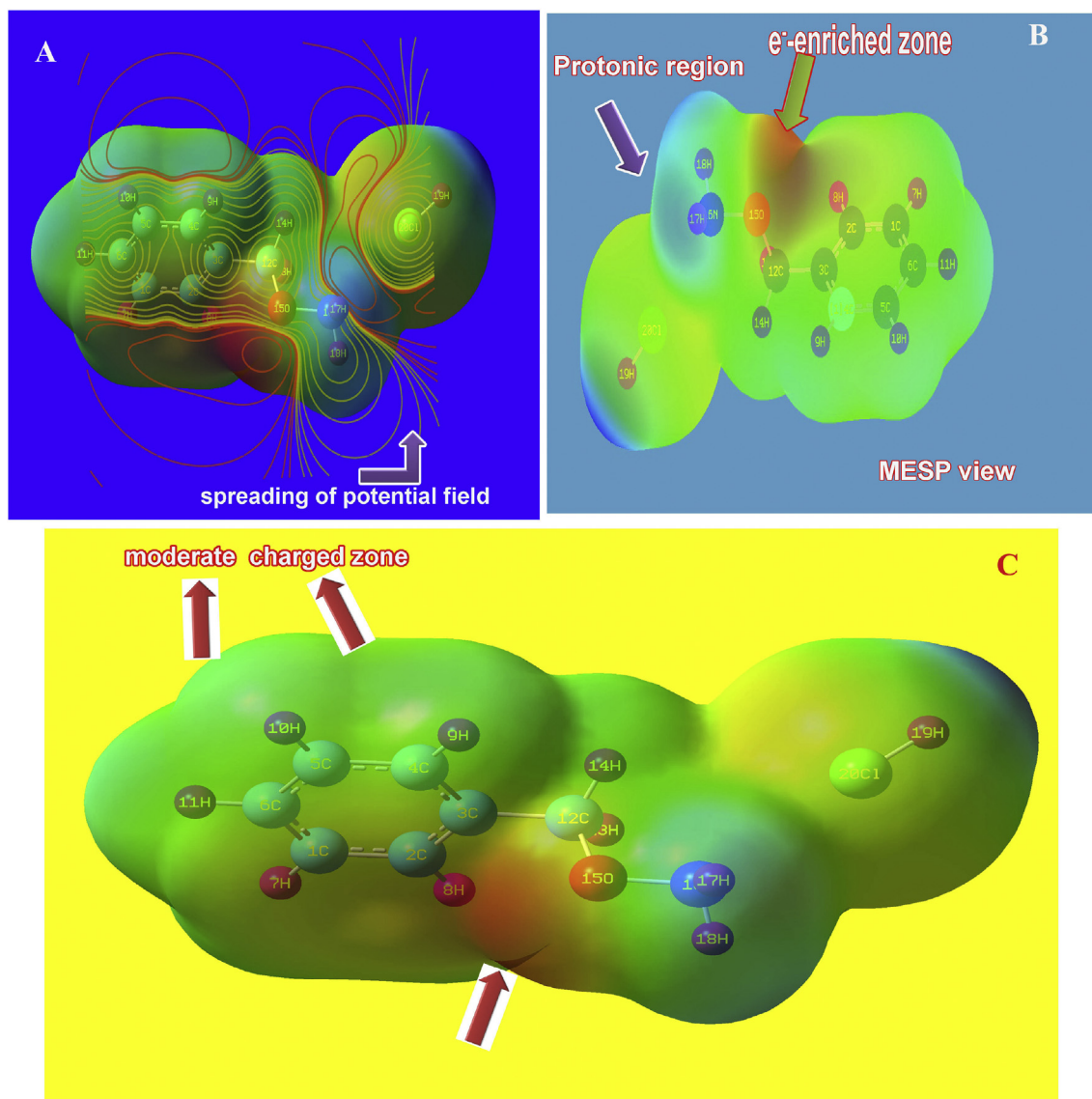| Parameters	B3LYP/6–311++G (d,p)	Parameters	B3LYP/6–311++G (d,p)
α_{xx}	-53.8786	β_{xxx}	72.1308
α_{xy}	1.0559	β_{xxy}	25.1519
α_{yy}	-64.3972	β_{xyy}	32.4619
α_{xz}	0.0757	β_{yyy}	-11.0358
α_{yz}	2.1437	β_{xxz}	-14.5590
α_{zz}	-64.6896	β_{xyz}	-22.9781
α_{tot}	144.833	β_{yyz}	2.5713
$\Delta\alpha$	194.028	β_{xzz}	19.4169
μ_x	1.1149	β_{yzz}	-3.6523
μ_y	0.3659	β_{zzz}	8.5432
μ_z	-0.1941	β_{totB}	294.21
μ_{tot}	1.1894		

Fig. 9. (A) Filed view, (B) Depletion view and (C) vector depleted view; MEP view of O-Benzyl Hydroxylamine.

Table 9
The calculated NBMO values of *O-Benzyl Hydroxylamine.*

Donor NBO (i)	Acceptor NBO (j)	Transitions	E (2) kcal/mol	E(j)-E(i) a.u.	F (i,j) a.u.
C1 – C2	C2 – C3	σ-σ*	3.28	1.28	0.058
C1 – C2	C3 – C12	σ-σ*	3.54	1.12	0.056
C1 – C6	C1 – C2	π-π*	2.74	1.28	0.053
C1 – C6	C5 – C6	π-π*	2.68	1.28	0.052
C1 – C6	C2 – C3	π-π*	20.35	0.29	0.069
C1 – C6	C4 – C5	σ-σ*	19.77	0.28	0.067
C1 – H7	C2 – C3	σ-σ*	3.66	1.10	0.057
C1 – H7	C5 – C6	σ-σ*	3.69	1.10	0.057
C2 – C3	C1 – C2	σ-σ*	3.02	1.27	0.056
C2 – C3	C3 – C4	π-π*	3.52	1.27	0.060
C2 – C3	C1 – C6	π-π*	20.64	0.28	0.068
C2 – C3	C4 – C5	π-π*	20.58	0.28	0.068
C3 – C4	C2 – C3	π-π*	3.52	1.27	0.060
C3 – C4	C4 – C5	π-π*	3.02	1.27	0.056
C4 – C5	C1 – C 6	σ-σ*	20.78	0.28	0.068
C4 – C5	C2 – C 3	σ-σ*	20.61	0.29	0.069
O15	C12 – H13	L-σ*	5.52	0.70	0.056
O15	C12 – H14	L-σ*	5.48	0.70	0.056

previous case [31] which dealt antibiotic properties, almost same amount of chemical potential exchange was observed. According which, in this case also, the antibiotic equivalent potential exchange was observed. So, it was concluded that, this present case, having antibiotic characteristics along with antiseptic property.

4.12. VCD graph analysis

The VCD spectra of drug aromatics are much sensitive to measure the asymmetrical sequence of vibrations of compositional parts in dichroic form which is used to characterize drug toxicity [32, 33]. The Asymmetrical displacement of absorption and transmission sequence pattern of present molecule was presented in Fig. 10. According to the figure, the asymmetrical sequence was found to be far infrared region which showed the low level wavenumber ligand vibrations. This may be due to the atomic placement in multiple planes and it will not produce any adverse effect. At mid IR region, the strong peak was represented the important ligand characteristics which showed the clear enantiomer property. Such type of strong intensive dichroic peak holds the mirror characteristics of chemical species. In the case of near IR region, the transmission peak was administrated the vibrational dichroism which showed the vibrational property of amino group. Usually, the chemical characteristics are
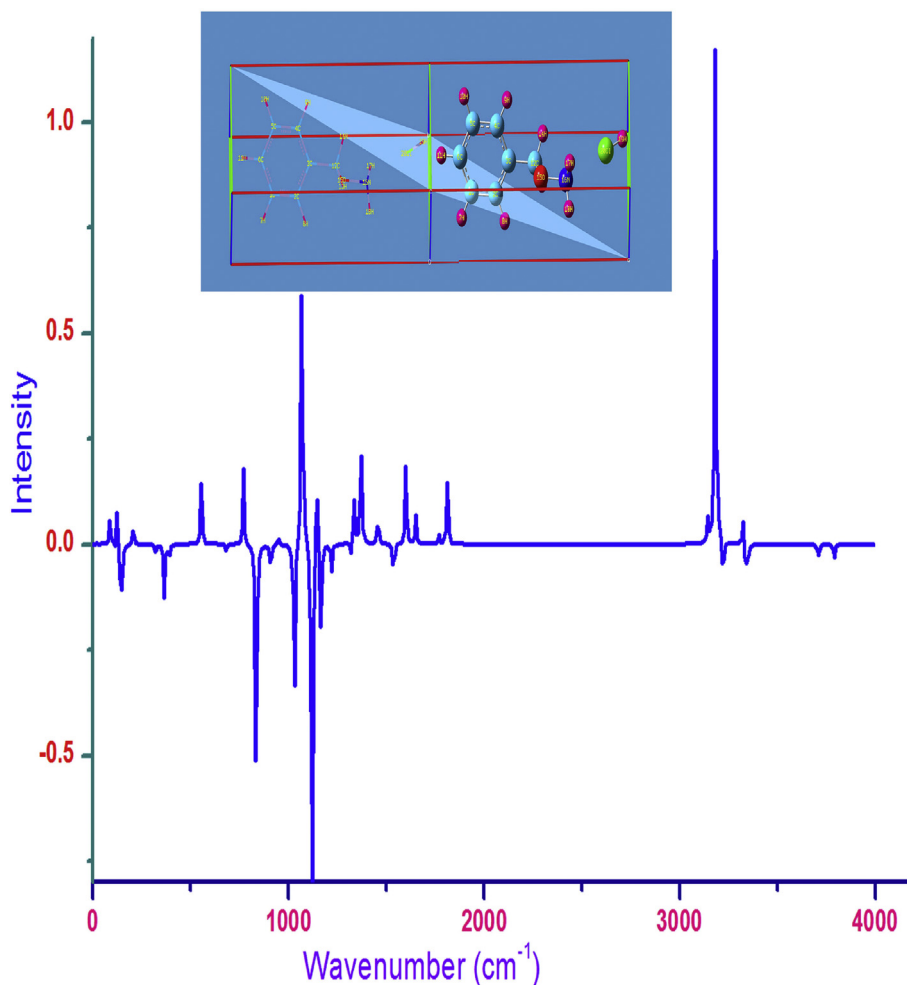
Fig. 10. VCD spectrum of O-Benzyl Hydroxylamine.

dominated by amino group present in the molecule and similarly, this group dominates in this case also. But, here, the end position of amino group, the vibrational dichroism showed contradictory enantiomer characteristics.

5. Conclusion

The aromatic drug species; O-Benzyl hydroxylamine was analyzed to explore drug, biological properties and hereby the antiseptic property was evaluated and validated. The molecular spectroscopic and theoretical tools with efficient method were used to carry out the investigation on molecular structural and vibrational characteristics. The atomic displacement on molecular site was monitored in order to explore the physical parameters evaluation to explain the physical characteristics. Asymmetrical dislocation of charge levels on ligand verses base compound was measured and the asymmetry of mulliken molecular electronic arrangement was monitored in order to find the cause of drug activity configuration. All the biological parameters were checked to expose the biological involvement of the present molecule. The Lipinski five rule validates the drug potential and enzyme inhibitor coefficient was tested to antiseptic intensiveness of the drug. The ligand group and base core participation in the structural properties in terms of vibrations were tested in different wavenumber region. The chemical reaction path was identified in the core carbo-bonds and the oscillation of the chemical potential around the molecule was monitored with the stipulations of chemical shift. The interconnected bond orbitals opened the nucleophilic and electrophilic interaction from which the degenerate orbital profile was studied to explore exact interactive bonding energy to induce drug activity. The non bonding partial energy exchange was measured for important molecular site and reason for inducement of antiseptic nature. The hyperactive pressure produced by the molecular multipole moments of the molecule for biological endurance was evaluated.

References

[1] Pediatrics 112 (6) (2003) 1394–1397.

[2] Katarzyna Blazewska, Tadeusz Gajda, *N*-(Diethoxyphosphoryl)-*O*-benzylhydroxylamine—a convenient substrate for the synthesis of *N*-substituted *O*-benzylhydroxylamines, Tetrahedron 59 (2003) 10249–10254.

[3] D.W. Knight, M.P. Leese, A survey of suitable protecting groups for the synthesis of hydroxylaminesby Mitsunobu reactions, Tetrahedron Lett. 42 (2001) 2593–2595.

[4] A. Bongini, G. Cardillo, L. Gentilucci, C. Tomasini, Synthesis of enantiomerically pure aziridine-2-imides by cyclization of chiral 3'-benzyloxyamino imide enolates, J. Org. Chem. 62 (1997) 9148–9153.

[5] D. Pettersen, M. Marcolini, L. Bernardi, F. Fini, R.P. Herrera, V. Sgarzani, A. Ricci, Direct access to enantiomerically enriched α-amino phosphonic acid derivatives by organocatalytic asymmetric hydrophosphonylation of imines, J. Org. Chem. 71 (2006) 6269–6272.

[6] A. Nikulin, P. Stern, Z. Zeger-Vidovic, The significance of histamine in the inflammation process, Arch. Znt. Pharmacodyn. 166 (1967) 305. PMID: 6032956.

[7] R.J. Levine, Histamine synthesis in man: inhibition by 4-bromo-3-hydroxybenzyloxyamine, Sci. N. Y. 154 (1966) 1017.

[8] F. Bessac, G. Frenking, Why is BCl_3 a stronger Lewis acid with respect to strong bases than BF3? Inorg. Chem. 42 (2003) 7990–8000.

[9] K. Morokuma, Molecular orbital studies of hydrogen bonds. III. C═O···H─O hydrogen bond in H_2CO···H_2O and H_2CO···$2H_2O$, J. Chem. Phys. 55 (1971) 1236.

[10] Peter Ertl, Bernhard Rohde, Paul Selzer, Fast calculation of molecular polar surface area as a sum of fragment-based contributions and its application to the prediction of drug transport properties, J. Med. Chem. 43 (20) (2000) 3714–3717.

[11] J.J. Irwin, D. Duan, H. Torosyan, A.K. Doak, K.T. Ziebart, T. Sterling, An aggregation advisor for ligand discovery, J. Med. Chem. 58 (17) (2015) 7076–7087.

[12] Shafqat Nadeem, Muhammad Sirajuddin, Saeed Ahmad, Syed Ahmed Tirmizi, Muhammad Irshad Ali, Abdul Hameed, Synthesis, spectral characterization and in vitro antibacterial evaluation and Petra/Osiris/Molinspiration analyses of new Palladium(II) iodide complexes with thioamides, Alexandria J. Med. 52 (3) (2016) 279–288.

[13] Dipshikha Sharma, Dipak Chetia, Mithun Rudrapal, Design, synthesis and antimalarial activity of some new 2-hydroxy-1,4-naphthoquinone-4-hydroxyaniline hybrid Mannich bases, Asian J. Chem. 28 (4) (2016) 782–788.

[14] Jag Mohan, Organic Spectroscopy: Principles and Applications, Narosa publishing House, New Delhi, 2004.

[15] G. Varsanyi, Vibrationai Spectra of Benzene Derivatives, Academic Press, New York, 1995.

[16] T.F. Ardyukova, et al., Atlas'Spectra for Aromatic and Heterocyclic Compounds, Nauka Sib. Otd., Novosibirsk, 1973.

[17] S.E. Wiberly, et al., Carbon-hydrogen stretching frequencies, Anal. Chem. 32 (1960) 217.

[18] A.R. Katritzky, P. Simmons, Infrared absorption of heteroaromatic and benzenoid six-membered monocylclic nuclei. Part VIII.-meta-disubstituted benzenes, J. Chem. Soc. (1959) 2058.

[19] A.R. Katritzky, J.M. Lagowski, Infrared absorption of heteroaromatic and benzenoid six-membered, monocyclic nuclei. Part IV. Monosubstituted benzenes, J. Chem. Soc. (1958) 4155.

[20] B. Chenon, C. Sandorfy, Hydrogen bonding in the amine hydrohalides: I. General aspects, Can. J. Chem. 36 (1958) 1181.

[21] Sikorski, Sanders, Reich, Tris(trimethylsilyl)methane as an internal ^{13}C NMR chemical shift thermometer, Magn. Reson. Chem. 36 (1998) S118.

[22] Sikorski Reich, Jones Sanders, J. Plessel, Multinuclear NMR study of the solution structure and reactivity of tris(trimethylsilyl)methyllithium and its iodine ate complex, Org. Chem. 74 (2009) 719–728.

[23] Kristin N. Plessel, Amanda C. Jones, Daniel J. Wherritt, Rebecca M. Maksymowicz, Eric T. Poweleit, Hans J. Reich, A rapid injection NMR study of the reaction of organolithium reagents with esters, amides, and ketones, Org. Lett. 17 (2015) 2310–2313.

[24] Nessreen A. Al-Hashimi, Yasser H.A. Hussein, Ab initio study on the formation of triiodide CT complex from the reaction of iodine with 2,3-diaminopyridine, Spectrochim. Acta, Part A 75 (2010) 198–202.

[25] M.A. Slifkin, Charge Transfer Interaction in Biomolecules, Academic Press, London, 1971.

[26] F.A. Bettelheim, Experimental Physical Chemistry, W.B. Saunders Co., Toronto, 1971.

[27] Jobann Gasteiger, Xinzhi Li, Christine Rudolph, Jens Sadowski, Jure Zupan, Representation of molecular electrostatic potentials by topological feature maps, J. Am. Chem. Soc. 116 (1994) 4608–4620.

[28] J. Zupn, Garlager, Neural networks: a new method for solving chemical problems or just a passing phase? J. Anal. Chim. Acta 248 (1991) 1–10.

[29] Jerome Berson, Chemical Creativity: Ideas from the Work of Woodward, Hückel, Meerwein, and Others, Wiley-VCH, New York, 1999.

[30] David Lewis, David Peters, Facts and Theories of Aromaticity, Macmillan Press, London, England, 1975.

[31] K. Hemachandran, P. Anbusrinivasan, S. Ramalingam, C. Manoharan, R. Aarthi, Biological and structural properties' interpretation on antitumour drug 3-(2-aminoethyl) indole (tryptamine) using molecular spectroscopy and computational tools, J. Taibah Univ. Sci. 13 (1) (2019) 231–247.

[32] Takeyuki Tanaka, Takashi S. Kodama, Hayato E. Morita, Takashi Ohno, Chirality, 18, Wiley Inter Science, 2006, pp. 652–661.

[33] W. Koch, M.C. Holthausen, A Chemist's Guide to Density Functional Theory, Wiley-VCH, Weinheim, 2000, p. 294.